Am J Physiol Cell Physiol 316: C649–C654, 2019.
First published March 6, 2019; doi:10.1152/ajpcell.00050.2019.

RAPID REPORT

Elevated myonuclear density during skeletal muscle hypertrophy in response to training is reversed during detraining

Cory M. Dungan,[1,3]* Kevin A. Murach,[1,3]* Kaitlyn K. Frick,[3] Savannah R. Jones,[3] Samuel E. Crow,[3] Davis A. Englund,[1,3] Ivan J. Vechetti, Jr.,[2,3] Vandre C. Figueiredo,[1,3] Bryana M. Levitan,[4] Jonathan Satin,[2] John J. McCarthy,[2,3] and Charlotte A. Peterson[1,3]

[1]*Department of Rehabilitation Sciences, University of Kentucky, Lexington, Kentucky;* [2]*Department of Physiology, University of Kentucky, Lexington, Kentucky;* [3]*Center for Muscle Biology, University of Kentucky, Lexington, Kentucky; and* [4]*Center for Molecular Medicine, University of Kentucky, Lexington, Kentucky*

Submitted 11 February 2019; accepted in final form 4 March 2019

Dungan CM, Murach KA, Frick KK, Jones SR, Crow SE, Englund DA, Vechetti IJ Jr, Figueiredo VC, Levitan BM, Satin J, McCarthy JJ, Peterson CA. Elevated myonuclear density during skeletal muscle hypertrophy in response to training is reversed during detraining. *Am J Physiol Cell Physiol* 316: C649–C654, 2019. First published March 6, 2019; doi:10.1152/ajpcell.00050.2019.—Myonuclei gained during exercise-induced skeletal muscle hypertrophy may be long-lasting and could facilitate future muscle adaptability after deconditioning, a concept colloquially termed "muscle memory." The evidence for this is limited, mostly due to the lack of a murine exercise-training paradigm that is nonsurgical and reversible. To address this limitation, we developed a novel progressive weighted-wheel-running (PoWeR) model of murine exercise training to test whether myonuclei gained during exercise persist after detraining. We hypothesized that myonuclei acquired during training-induced hypertrophy would remain following loss of muscle mass with detraining. Singly housed female C57BL/6J mice performed 8 wk of PoWeR, while another group performed 8 wk of PoWeR followed by 12 wk of detraining. Age-matched sedentary cage-dwelling mice served as untrained controls. Eight weeks of PoWeR yielded significant plantaris muscle fiber hypertrophy, a shift to a more oxidative phenotype, and greater myonuclear density than untrained mice. After 12 wk of detraining, the plantaris muscle returned to an untrained phenotype with fewer myonuclei. A finding of fewer myonuclei simultaneously with plantaris deconditioning argues against a muscle memory mechanism mediated by elevated myonuclear density in primarily fast-twitch muscle. PoWeR is a novel, practical, and easy-to-deploy approach for eliciting robust hypertrophy in mice, and our findings can inform future research on the mechanisms underlying skeletal muscle adaptive potential and muscle memory.

exercise; muscle memory; myonuclear accretion; satellite cell; weighted-wheel running

INTRODUCTION

Skeletal muscle fibers are believed to possess a "memory" of previous exercise exposure, where prior adaptation facilitates future adaptability (5, 11, 15, 22). One hypothesis is that myonuclei gained from exercise-induced hypertrophy are long-lasting or permanent and that the maintenance of elevated myonuclear density, once hypertrophy is reversed, constitutes a "muscle memory" mechanism (5, 11, 15). Support for this hypothesis was first provided in 2010 by Bruusgaard et al. (4), who employed synergist ablation surgery on the tibialis anterior muscle in mice to induce hypertrophy of the extensor digitorum longus (EDL) muscle followed by denervation to cause subsequent atrophy. The EDL is a small non-load-bearing toe extensor comprising primarily type IIb muscle fibers (2), and atrophy via nerve damage is unique because it may result in elevated protein synthesis (1, 10, 14); therefore, it is likely that denervation following hypertrophy is distinct from detraining after exercise training. Under these unique conditions in the EDL muscle, nuclei gained from surgical overload remained after denervation, resulting in muscle fibers that were hypernucleated per unit size (4). Follow-up investigations in mice (5) and rats (15) provide further evidence that myonuclei gained following hypertrophy of fast-twitch muscles controlling toe extension and flexion are permanent and that the additional myonuclei confer some future benefit for hypertrophic adaptation. A myonuclear density-mediated muscle memory is provocative but remains to be convincingly supported in the context of exercise-induced hypertrophy and detraining.

In this investigation we describe a progressive weighted-wheel-running (PoWeR) protocol for inducing hypertrophy in the plantaris muscles of mice. PoWeR is advantageous relative to other murine hypertrophy models, such as synergist ablation, because it involves the modification of standard running wheels using readily available hardware, is nonsurgical, allows for the reversibility of adaptation in a load-bearing plantar flexor muscle, and approximates exercise training in humans. Concomitant with hypertrophy, PoWeR elicits myonuclear accretion measured by two distinct detection methods, as well as a shift from a fast to a slower fiber type. By leveraging the ability to detrain from PoWeR, we hypothesized that myonuclei acquired during hypertrophy would remain after 3 mo of detraining (>10% of murine lifespan), whereas other training adaptations would be lost.

MATERIALS AND METHODS

Ethical approval. All animal procedures were approved by the Institutional Animal Care and Use Committee of the University of Kentucky. Mice were housed in a temperature- and humidity-controlled room, maintained on a 14:10-h light-dark cycle, and allowed ad libitum

* C. M. Dungan and K. A. Murach are co-first authors.
Address for reprint requests and other correspondence: C. A. Peterson, Rm. 439 Wethington Bldg., 900 South Limestone St., Lexington, KY 40536 (e-mail: cpete4@uky.edu).

access to food and water. Animals were euthanized via a lethal dose of pentobarbital sodium injected intraperitoneally followed by cervical dislocation.

Experimental design. Female C57BL/6J mice (≥4 mo old, <35 g body wt) were obtained from The Jackson Laboratory (Bar Harbor, ME). Mice were assigned to groups as follows: 8 wk of PoWeR (PoWeR group, $n = 9$), 8 wk of PoWeR followed by 12 wk of detraining (detrained group, $n = 8$), 6-mo-old untrained controls age-matched to the PoWeR group (6-mo untrained group, $n = 10$), and 9-mo-old untrained controls age-matched to the detraining group (9-mo untrained group, $n = 6$). Mice were housed singly during PoWeR for monitoring of individual running speed (km/h), total distance run (km/day), and total time run (h/day), which were recorded using ClockLab software (Actimetrics, Wilmette, IL). After 1 wk of acclimation to an unweighted wheel, 8 wk of PoWeR consisted of 2 g of weight in *week 1*, 3 g in *week 2*, 4 g in *week 3*, 5 g in *weeks 4* and *5*, and 6 g in *weeks 6–8* (Fig. 1*A*). The wheels were loaded with 1-g magnets (product no. B661, K&J Magnetics, Pipersville, PA), which were affixed in one location along the outside circumference (Fig. 1*A*, *inset*). The asymmetric weighting strategy resulted in an unbalanced wheel, in contrast to the friction-based continual loading of traditional weighted wheels that becomes difficult for a mouse to overcome as the weight increases. The momentum of the wheel also caused the mice to misstep and briefly discontinue running on a frequent basis, thereby forcing intermittent rest periods. To resume running, the mice repeatedly

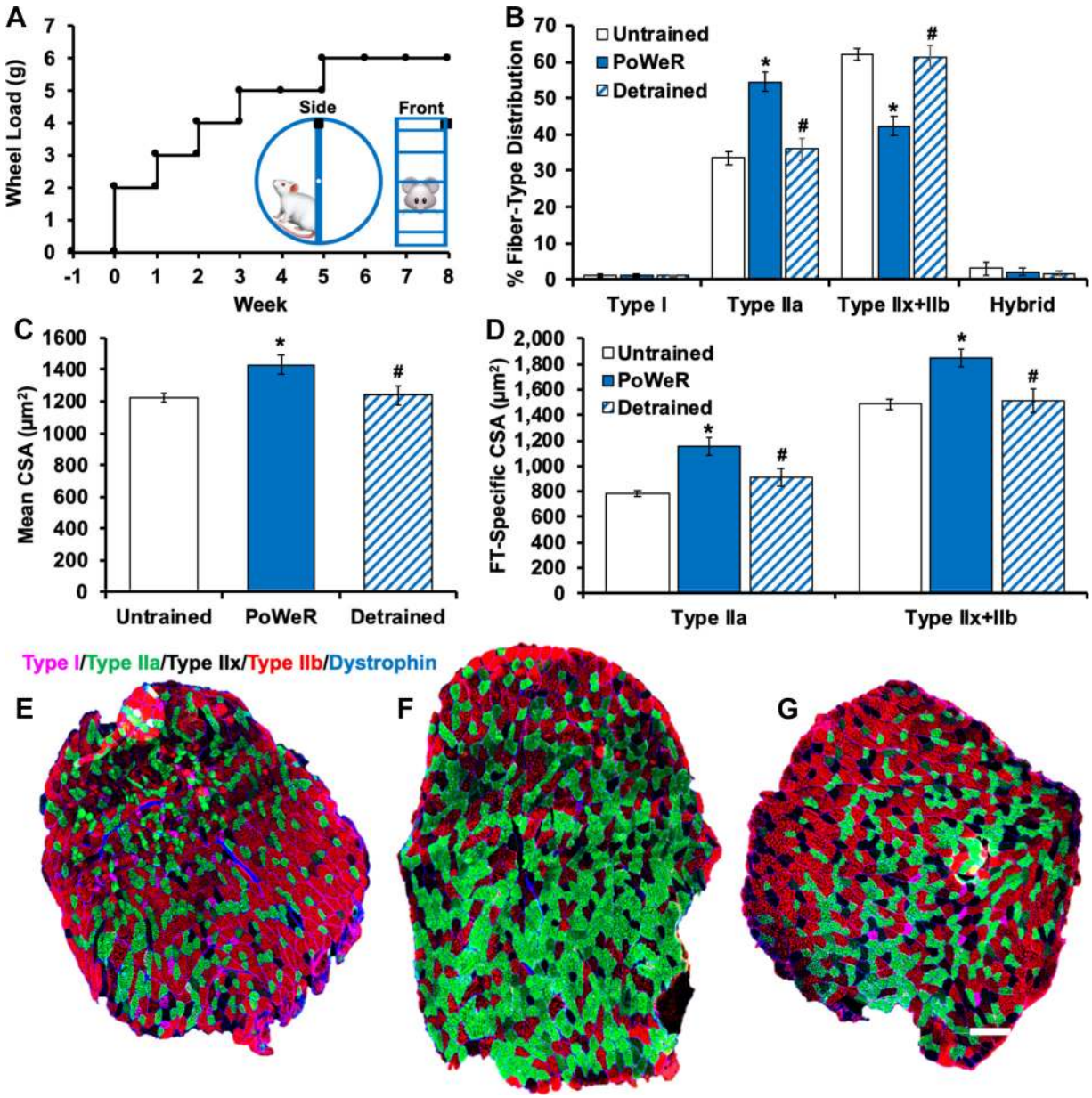

Fig. 1. Muscle fiber type and size adaptations to progressive weighted-wheel-running (PoWeR) training and detraining. *A*: PoWeR wheel-loading strategy. *Inset*: magnet (black box) placement on the wheel. *B*: fiber type distribution data for untrained ($n = 14$), PoWeR-trained ($n = 8$), and detrained ($n = 7$) mice. *C*: average muscle fiber cross-sectional area (CSA) in untrained, PoWeR-trained, and detrained mice. *D*: fiber type (FT)-specific CSA data for untrained, PoWeR-trained, and detrained mice. Values are means ± SE. *$P < 0.05$ vs. untrained; #$P < 0.05$ vs. PoWeR-trained. *E–G*: representative images of fiber type and dystrophin staining on entire muscle cross sections from untrained (*E*), PoWeR-trained (*F*), and detrained (*G*) mice. Pink, type I; green, type IIa; red, type IIb; unstained/black, type IIx; blue, dystrophin. Scale bar = 200 μm.

overcame the weight of the wheel, providing an additional resistive component to the training.

Echocardiography. Transthoracic echocardiography was performed using a VisualSonics 3100 imaging system (Toronto, ON, Canada). Analysis was performed under light anesthesia (1–2% inhaled isoflurane), with heart rate continuously monitored (350–500 beats/min). Left ventricular dimensions and calculated left ventricular ejection fraction were measured from the short-axis M-mode display. All measurements were obtained in triplicate and averaged, and the sonographer was blinded to experimental conditions.

Immunohistochemistry. Immunohistochemistry (IHC) analysis of plantaris muscles was performed as previously described by our laboratory using antibodies that are well established as specific (6, 7, 21). For fiber type distribution, overall muscle fiber cross-sectional area (CSA), fiber type-specific CSA, and myonuclear density, frozen sections were incubated overnight in a cocktail of isotype-specific anti-mouse primary antibodies for myosin heavy chain (MyHC) I, MyHC IIa, MyHC IIb, or embryonic MyHC (Developmental Studies Hybridoma Bank, Iowa City, IA), along with an antibody against dystrophin (1:100 dilution; catalog no. ab15277, Abcam, St. Louis, MO), incubated in the appropriate secondary antibodies, and then mounted using VectaShield with DAPI (Vector Laboratories). Some mice were excluded from certain analyses due to insufficient quality for automated software detection (25). IHC for $Pax7^+$ satellite cells was performed according to the established protocol from our laboratory (6, 7, 17, 21).

Single muscle fiber myonuclear analysis. Myonuclei on isolated single muscle fibers were counted as previously described by our laboratory and others (3, 17, 21). The mechanical/chemical separation of individual fibers reduces the influence of nonmyonuclei contributing to myonuclear counts and accounts for any potential influences of myonuclear shape changes. Briefly, plantaris muscles were fixed in situ at resting length in 4% paraformaldehyde for 48 h to control for sarcomere spacing. Muscle fibers were liberated by NaOH incubation, pipetted onto glass slides, and then mounted using VectaShield with DAPI (Vector Laboratories). Thirty fibers per muscle per mouse (~300- to 500-μm random linear segments per individual fiber) were used for myonuclear density analysis (21).

Image capture and analysis. For IHC, images were captured at ×20 magnification using an upright fluorescence microscope (AxioImager M1, Zeiss, Oberkochen, Germany). Whole muscle sections were obtained using the mosaic function in Zeiss Zen 2.3. Quantification of entire cross sections eliminates the possibility of misrepresentation due to the regional nature of skeletal muscles and accounts for the potential effects of increased fiber number via de novo muscle fiber formation and/or fiber splitting (19, 21). Everything but satellite cells was quantified on entire muscle cross sections using MyoVision automated analysis software (25). Specifically, quantification of myonuclei per fiber on entire cross sections using DAPI/dystrophin provides a comprehensive picture of hundreds of fibers, and automated analysis eliminates bias and enhances validity of this potentially subjective measure. Satellite cells ($Pax7^+$/$DAPI^+$) were counted manually and normalized to fiber number. For single-fiber myonuclear analysis, fibers were imaged at ×20 magnification using the *z*-stack function within the Zen software (21). All manual counting was performed by a blinded, trained technician.

Statistics. Data were checked for normality, and original or log-transformed mean data were used for analysis. Differences between untrained control/age-matched control, 8-wk PoWeR, and detraining groups were detected using a one-way ANOVA combined with Tukey's post hoc tests. Significance was set at $P < 0.05$. Data points that were 1.5 interquartile ranges below the first quartile or above the third quartile were considered outliers and were removed from the analysis.

RESULTS

Voluntary exercise performance was maintained during 8 wk of PoWeR training. In contrast to other reports of weighted-wheel running (12, 13, 24, 26), there was no appreciable decline in running distance during PoWeR training (Table 1). The systemic effect of PoWeR training is evidenced by the marked increase in heart mass (Table 1) and left ventricular wall thickness (Table 1) after 8 wk.

Plantaris skeletal muscle mass was greater following 8 wk of PoWeR training and less following 12 wk of detraining. Muscle wet weights relative to body weight were significantly greater in mice after 8 wk of PoWeR training than in untrained control (6 mo old) and detrained mice (Table 1). Nine-month-old untrained control mice were compared with 9-mo-old detrained mice. Normalized muscle wet weight was not different between detrained mice and 9-mo-old untrained controls. Furthermore, muscle weight, muscle fiber size, and myonuclear density were not different between 6- and 9-mo-old untrained mice (see below). For these reasons, control groups were collapsed for further analyses.

PoWeR training resulted in fiber type adaptations that were reversed after detraining. A significant shift toward a more oxidative fiber type profile in the plantaris muscle (types IIx and IIb → type IIa; Fig. 1*B*) was observed after 8 wk of PoWeR training. Fiber type distribution reverted to an untrained phenotype following 12 wk of detraining (type IIa → types IIx and IIb; Fig. 1*B*). Embryonic MyHC expression, a marker of regeneration, was not observed at any time point in any group (data not shown), nor was muscle fiber number different across conditions (data not shown). Centrally located myonuclei, another hallmark of muscle regeneration, were rare but slightly

Table 1. Mouse characteristics

	Untrained			
	6 mo old	9 mo old	PoWeR	Detrained
Body wt, g	23.1 ± 0.5[a]	27.4 ± 0.7[b]	23.7 ± 0.3[a]	29.7 ± 0.9[b]
Normalized plantaris wt, mg/g	0.50 ± 0.01[a]	0.50 ± 0.02[a]	0.58 ± 0.02[b]	0.41 ± 0.01[c]
Normalized heart wt, mg/g	6.6 ± 0.5[a]	6.1 ± 0.2[a]	8.8 ± 0.2[b]	5.9 ± 0.3[a]
Resting heart rate, beats/min	447.8 ± 11.7[a]	n/a	412.0 ± 8.7[b]	n/a
Ejection fraction, %	64.9 ± 1.8[a]	n/a	58.3 ± 1.1[b]	n/a
LV internal diameter (end diastole), mm	3.7 ± 0.1[a]	n/a	4.1 ± 0.1[b]	n/a
LV anterior wall (end diastole), mm	0.92 ± 0.09[a]	n/a	0.91 ± 0.04[a]	n/a
LV posterior wall (end diastole), mm	0.80 ± 0.04[a]	n/a	0.92 ± 0.03[b]	n/a
Distance run, km/day	n/a	n/a	12.5 ± 0.8[a]	12.3 ± 1.4[a]

Values are means ± SE. LV, left ventricular; n/a, not applicable; PoWeR, progressive weighted-wheel running.[a,b,c]Groups that share a letter designation for a given outcome are not significantly different.

elevated following 8 wk of PoWeR training in the plantaris muscle (~1% of fibers in untrained and ~2% with PoWeR; data not shown); these values are notably less than the 9% centrally nucleated muscle fibers in the plantaris muscle 8 wk after synergist ablation (7). The rare centrally nucleated muscle fibers and the absence of embryonic MyHC-expressing fibers suggest that PoWeR is a less damaging model than synergist ablation for inducing hypertrophy in mice.

Muscle fiber CSA was greater in PoWeR-trained than untrained and detrained mice. Mean (17%; Fig. 1*C*) and fiber type-specific (47% type IIa and 24% types IIx and IIb; Fig. 1*D*) CSA in the plantaris muscle was greater in PoWeR-trained than untrained mice. Muscle fiber CSA was 16% lower in detrained than PoWeR-trained mice (Fig. 1*C*) and not different from untrained mice. Fiber type and dystrophin IHC representative images of whole muscle cross sections from an untrained, a PoWeR-trained, and a detrained mouse are displayed in Fig. 1, *E–G*.

Myonuclear and satellite cell density was elevated in PoWeR-trained mice and was the same as in untrained mice following detraining. We utilized two methods to quantify myonuclei per fiber: *1*) manual counting of DAPI-stained myonuclei on fixed isolated single muscle fibers (>150 individual fiber segments per group) and *2*) DAPI/dystrophin IHC on entire muscle cross sections (>300 fibers per muscle section, ≥1 section per mouse) quantified via automated analysis software (25). We observed 27% and 33% greater myonuclear density in PoWeR-trained (Fig. 2*A–F*) than untrained mouse muscles via single-fiber and cross-sectional analysis, respectively. As myonuclear accretion is mediated by the fusion of muscle stem cells ($Pax7^+$ satellite cells), we found a correspondingly greater satellite cell abundance in PoWeR-trained mice (44%; Fig. 2, *G* and *H*). After 12 wk of detraining, both myonuclear (Fig. 2, *A–F*) and satellite cell (Fig. 2, *G* and *H*) density were comparable to untrained values.

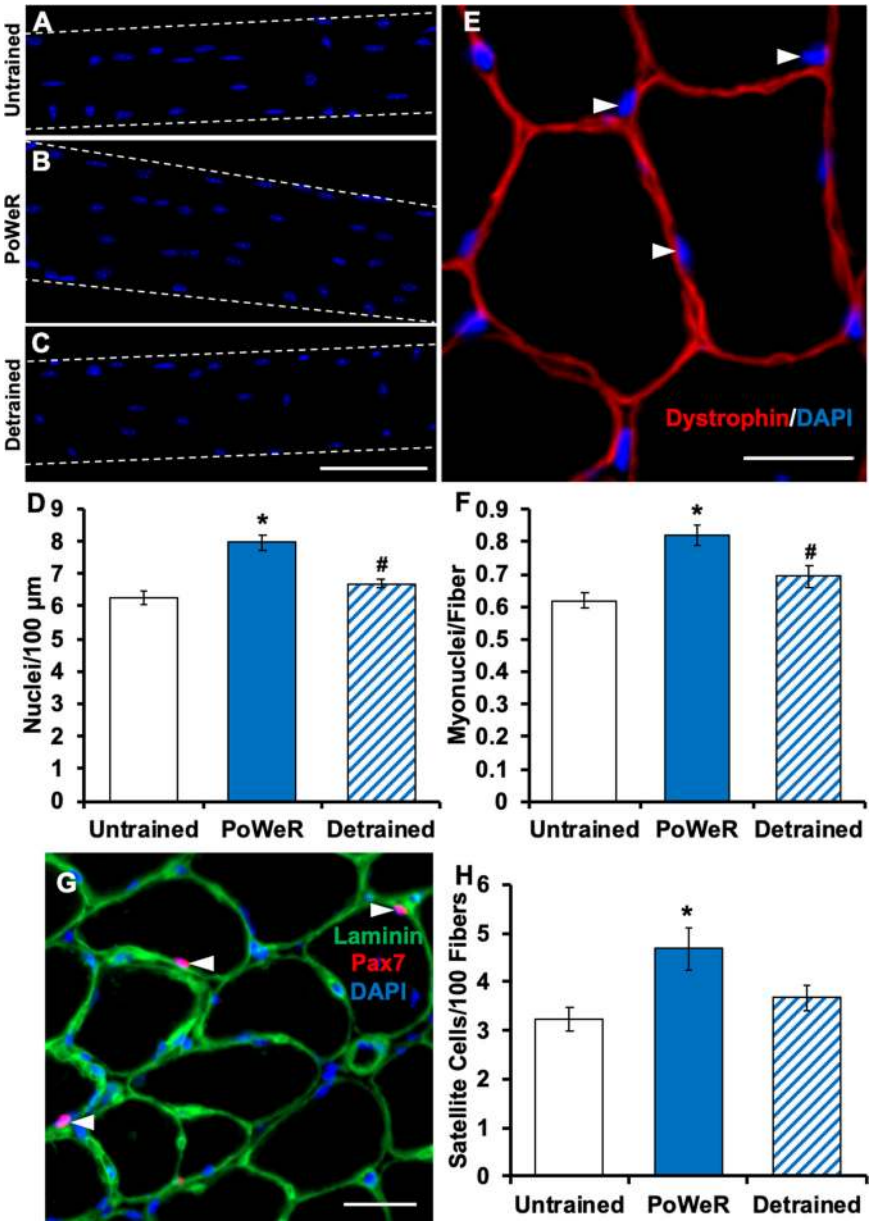

Fig. 2. Myonuclear and satellite cell density adaptations to progressive weighted-wheel-running (PoWeR) training and detraining. *A–C*: representative images of longitudinal muscle fibers and myonuclei in untrained, PoWeR-trained, and detrained mice. Blue, $DAPI^+$ myonuclei. Scale bar = 100 μm. *D*: single-fiber myonuclear density data analysis for untrained (n = 8), PoWeR-trained (n = 7), and detrained mice (n = 8). *E*: representative image of dystrophin and DAPI staining for immunohistochemical (IHC) myonuclear density analysis. Red, dystrophin; blue, DAPI. White arrows point to myonuclei. Scale bar = 20 μm. *F*: IHC myonuclear density analysis for untrained (n = 10), PoWeR-trained (n = 7), and detrained (n = 6) mice. *G*: representative image of IHC satellite cell identification. Green, laminin; blue, DAPI; pink, Pax7. White arrows point to $Pax7^+$/$DAPI^+$ satellite cells located beneath the laminin border. Scale bar = 50 μm. *H*: satellite cell density in untrained (n = 14), PoWeR-trained (n = 7), and detrained (n = 8) mice. Values are means ± SE. *P < 0.05 vs. untrained; #P < 0.05 vs. PoWeR-trained.

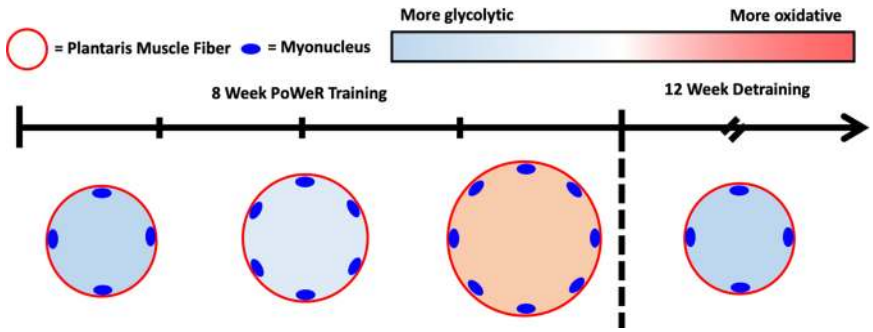

Fig. 3. Schematic illustrating muscle fiber adaptations to progressive weighted-wheel running (PoWeR) and detraining.

DISCUSSION

PoWeR, a practical, nonsurgical, and highly effective strategy for inducing robust adaptations in murine skeletal muscle, enables the study of muscle response following the return to sedentary conditions. We found greater muscle fiber size and myonuclear density in mice subjected to 8 wk of PoWeR training than in untrained controls but a return to untrained values following 12 wk of detraining (>10% of mouse lifespan; Fig. 3). Our data challenge the concept that muscle fibers have a memory of previous hypertrophy that is governed by myonuclei acquired from training, at least in the fast-twitch plantaris muscle of mice.

PoWeR training is a translatable model for the study of skeletal muscle hypertrophy in mice. Similar to cycling or combined endurance and resistance exercise training in humans (8, 18, 20), volitional PoWeR results in whole muscle and muscle fiber hypertrophy, a transition from a fast to a slower fiber type, myonuclear accretion, and cardiac adaptations. The classic model for studying skeletal muscle hypertrophy in rodent models is the synergist ablation surgical method (9), but this approach in mice has limitations: *1*) the surgery is stressful, and overload can cause degeneration/regeneration, *2*) the rate of hypertrophy exceeds that observed with resistance training in humans, *3*) hypertrophy is not reversible without unloading or denervation, and *4*) overload is a continual stimulus that is unlike episodic exercise training in humans. Instead, PoWeR exploits the mouse's natural inclination for periodic high activity levels and circumvents the aforementioned issues. A shortcoming of previous weighted-wheel-running approaches was that the progression of loading was too rapid and the constant wheel loading was too great for the mice to run at a sustainable pace, collectively discouraging continued exercise (12, 13, 24, 26). We speculate that the unbalanced running wheel and variable resistance used in PoWeR encourages continued exercise and facilitates the marked adaptations observed here.

Myonuclear density is the same in untrained and detrained muscle. Using synergist ablation overload followed by denervation in mice, Bruusgaard et al. first postulated that myonuclei gained during hypertrophy in a small dorsiflexor muscle were permanent and represented a muscle memory of previous adaptation (4). In contrast, using fully mature adult (>4 mo old) mice combined with hypertrophy and deconditioning that do not involve surgical overload (4, 5), denervation (4), or anabolic steroids (5), we show that myonuclear density in a comparatively larger load-bearing plantar flexor muscle is the same in detrained and untrained conditions; we verified this using two different methods of myonuclear density quantification. A recent resistance-training study in rats found that myonuclei density was the same in untrained and detrained muscle (15), but the results are difficult to interpret. The rats began training at a young age (8 wk), when developmental muscle growth was ongoing, which could affect how myonuclear accretion contributes to hypertrophy (16). For instance, our laboratory has shown that young growing mice have a strict requirement for myonuclear accretion during hypertrophy, whereas mature adult mice do not (21); this may have implications for myonuclear requirements and stability during detraining and retraining. Furthermore, myonuclear density in the rat study was obtained from a small number of isolated fibers (5–11 per muscle). Although neuromuscular adaptations cannot be ruled out, we agree with Sharples and colleagues in that epigenetic modifications within myonuclei (i.e., DNA methylation, histone methylation, or acetylation) (22, 23), and not long-lasting alterations in myonuclear number (11), may contribute to potential muscle memory mechanisms of previous hypertrophy that influence future muscle adaptability.

Physiological significance. PoWeR is a practical tool for inducing hypertrophy in murine skeletal muscle and can be used to explore the mechanisms of exercise-induced hypertrophy, deconditioning, and reconditioning. Since the increase in myonuclear density acquired by loading-induced muscle hypertrophy is not sustained after deconditioning in the plantaris muscle, it may be prudent to expand the search for the mechanism(s) mediating the augmented growth response that has been documented during retraining (22). Future investigations will aim to elucidate cell-autonomous mechanisms mediating a muscle memory, how myonuclei are lost during detraining, and the extent to which resident or satellite cell-derived myonuclei are targeted for removal.

ACKNOWLEDGMENTS

The authors thank Laura Peterson Brown, Dr. Yuan Wen, and Dr. Sarah White for assistance on this project.

GRANTS

Funding for this study was provided by National Institutes of Health Grants AR-071753 (to K. A. Murach), AR-060701 and AG-049806 (to C. A. Peterson and J. J. McCarthy), and AG-046920 (to C. A. Peterson).

DISCLOSURES

No conflicts of interest, financial or otherwise, are declared by the authors.

AUTHOR CONTRIBUTIONS

C.M.D., J.J.M., and C.A.P. conceived and designed research; C.M.D., K.A.M., K.K.F., S.R.J., S.E.C., D.A.E., I.J.V., V.C.F., and B.M.L. performed

experiments; C.M.D., K.A.M., K.K.F., S.R.J., S.E.C., D.A.E., I.J.V., V.C.F., and B.M.L. analyzed data; C.M.D., K.A.M., and J.S. interpreted results of experiments; C.M.D. prepared figures; C.M.D. and K.A.M. drafted manuscript; C.M.D., K.A.M., D.A.E., J.S., J.J.M., and C.A.P. edited and revised manuscript; C.M.D., K.A.M., K.K.F., S.R.J., S.E.C., D.A.E., I.J.V., V.C.F., B.M.L., J.S., J.J.M., and C.A.P. approved final version of manuscript.

REFERENCES

1. **Argadine HM, Hellyer NJ, Mantilla CB, Zhan W-Z, Sieck GC.** The effect of denervation on protein synthesis and degradation in adult rat diaphragm muscle. *J Appl Physiol (1985)* 107: 438–444, 2009. doi:10.1152/japplphysiol.91247.2008.
2. **Bloemberg D, Quadrilatero J.** Rapid determination of myosin heavy chain expression in rat, mouse, and human skeletal muscle using multicolor immunofluorescence analysis. *PLoS One* 7: e35273, 2012. doi:10.1371/journal.pone.0035273.
3. **Brack AS, Bildsoe H, Hughes SM.** Evidence that satellite cell decrement contributes to preferential decline in nuclear number from large fibres during murine age-related muscle atrophy. *J Cell Sci* 118: 4813–4821, 2005. doi:10.1242/jcs.02602.
4. **Bruusgaard JC, Johansen IB, Egner IM, Rana ZA, Gundersen K.** Myonuclei acquired by overload exercise precede hypertrophy and are not lost on detraining. *Proc Natl Acad Sci USA* 107: 15111–15116, 2010. doi:10.1073/pnas.0913935107.
5. **Egner IM, Bruusgaard JC, Eftestøl E, Gundersen K.** A cellular memory mechanism aids overload hypertrophy in muscle long after an episodic exposure to anabolic steroids. *J Physiol* 591: 6221–6230, 2013. doi:10.1113/jphysiol.2013.264457.
6. **Fry CS, Kirby TJ, Kosmac K, McCarthy JJ, Peterson CA.** Myogenic progenitor cells control extracellular matrix production by fibroblasts during skeletal muscle hypertrophy. *Cell Stem Cell* 20: 56–69, 2017. doi:10.1016/j.stem.2016.09.010.
7. **Fry CS, Lee JD, Jackson JR, Kirby TJ, Stasko SA, Liu H, Dupont-Versteegden EE, McCarthy JJ, Peterson CA.** Regulation of the muscle fiber microenvironment by activated satellite cells during hypertrophy. *FASEB J* 28: 1654–1665, 2014. doi:10.1096/fj.13-239426.
8. **Fry CS, Noehren B, Mula J, Ubele MF, Westgate PM, Kern PA, Peterson CA.** Fibre type-specific satellite cell response to aerobic training in sedentary adults. *J Physiol* 592: 2625–2635, 2014. doi:10.1113/jphysiol.2014.271288.
9. **Goldberg AL.** Work-induced growth of skeletal muscle in normal and hypophysectomized rats. *Am J Physiol* 213: 1193–1198, 1967. doi:10.1152/ajplegacy.1967.213.5.1193.
10. **Goldspink DF.** The effects of denervation on protein turnover of rat skeletal muscle. *Biochem J* 156: 71–80, 1976. doi:10.1042/bj1560071.
11. **Gundersen K.** Muscle memory and a new cellular model for muscle atrophy and hypertrophy. *J Exp Biol* 219: 235–242, 2016. doi:10.1242/jeb.124495.
12. **Ishihara A, Hirofuji C, Nakatani T, Itoh K, Itoh M, Katsuta S.** Effects of running exercise with increasing loads on tibialis anterior muscle fibres in mice. *Exp Physiol* 87: 113–116, 2002. doi:10.1113/eph8702340.
13. **Konhilas JP, Widegren U, Allen DL, Paul AC, Cleary A, Leinwand LA.** Loaded wheel running and muscle adaptation in the mouse. *Am J Physiol Heart Circ Physiol* 289: H455–H465, 2005. doi:10.1152/ajpheart.00085.2005.
14. **Langer HT, Senden JMG, Gijsen AP, Kempa S, van Loon LJC, Spuler S.** Muscle atrophy due to nerve damage is accompanied by elevated myofibrillar protein synthesis rates. *Front Physiol* 9: 1220, 2018. doi:10.3389/fphys.2018.01220.
15. **Lee H, Kim K, Kim B, Shin J, Rajan S, Wu J, Chen X, Brown MD, Lee S, Park JY.** A cellular mechanism of muscle memory facilitates mitochondrial remodelling following resistance training. *J Physiol* 596: 4413–4426, 2018. doi:10.1113/JP275308.
16. **McCarthy JJ, Dupont-Versteegden EE, Fry CS, Murach KA, Peterson CA.** Methodological issues limit interpretation of negative effects of satellite cell depletion on adult muscle hypertrophy. *Development* 144: 1363–1365, 2017. doi:10.1242/dev.145797.
17. **McCarthy JJ, Mula J, Miyazaki M, Erfani R, Garrison K, Farooqui AB, Srikuea R, Lawson BA, Grimes B, Keller C, Van Zant G, Campbell KS, Esser KA, Dupont-Versteegden EE, Peterson CA.** Effective fiber hypertrophy in satellite cell-depleted skeletal muscle. *Development* 138: 3657–3666, 2011. doi:10.1242/dev.068858.
18. **Murach KA, Bagley JR.** Skeletal muscle hypertrophy with concurrent exercise training: contrary evidence for an interference effect. *Sports Med* 46: 1029–1039, 2016. doi:10.1007/s40279-016-0496-y.
19. **Murach KA, Dungan CM, Peterson CA, McCarthy JJ.** Muscle fiber splitting is a physiological response to extreme loading in animals. *Exerc Sport Sci Rev* 47: 108–115, 2019. doi:10.1249/JES.0000000000000181. 30640746
20. **Murach KA, Walton RG, Fry CS, Michaelis SL, Groshong JS, Finlin BS, Kern PA, Peterson CA.** Cycle training modulates satellite cell and transcriptional responses to a bout of resistance exercise. *Physiol Rep* 4: e12973, 2016. doi:10.14814/phy2.12973.
21. **Murach KA, White SH, Wen Y, Ho A, Dupont-Versteegden EE, McCarthy JJ, Peterson CA.** Differential requirement for satellite cells during overload-induced muscle hypertrophy in growing versus mature mice. *Skelet Muscle* 7: 14, 2017. doi:10.1186/s13395-017-0132-z.
22. **Seaborne RA, Strauss J, Cocks M, Shepherd S, O'Brien TD, van Someren KA, Bell PG, Murgatroyd C, Morton JP, Stewart CE, Sharples AP.** Human skeletal muscle possesses an epigenetic memory of hypertrophy. *Sci Rep* 8: 1898, 2018. doi:10.1038/s41598-018-20287-3.
23. **Sharples AP, Stewart CE, Seaborne RA.** Does skeletal muscle have an 'epi'-memory? The role of epigenetics in nutritional programming, metabolic disease, aging and exercise. *Aging Cell* 15: 603–616, 2016. doi:10.1111/acel.12486.
24. **Soffe Z, Radley-Crabb HG, McMahon C, Grounds MD, Shavlakadze T.** Effects of loaded voluntary wheel exercise on performance and muscle hypertrophy in young and old male C57Bl/6J mice. *Scand J Med Sci Sports* 26: 172–188, 2016. doi:10.1111/sms.12416.
25. **Wen Y, Murach KA, Vechetti IJ Jr, Fry CS, Vickery C, Peterson CA, McCarthy JJ, Campbell KS.** MyoVision: software for automated high-content analysis of skeletal muscle immunohistochemistry. *J Appl Physiol (1985)* 124: 40–51, 2018. doi:10.1152/japplphysiol.00762.2017.
26. **White Z, Terrill J, White RB, McMahon C, Sheard P, Grounds MD, Shavlakadze T.** Voluntary resistance wheel exercise from mid-life prevents sarcopenia and increases markers of mitochondrial function and autophagy in muscles of old male and female C57BL/6J mice. *Skelet Muscle* 6: 45, 2016. [Erratum in *Skelet Muscle* 7: 4, 2017.] doi:10.1186/s13395-016-0117-3.